BIOENGINEERED
2021, VOL. 12, NO. 1, 2352–2363
https://doi.org/10.1080/21655979.2021.1935401

Taylor & Francis
Taylor & Francis Group

RESEARCH PAPER

OPEN ACCESS Check for updates

Correlation and integration of circulating miRNA and peripheral whole blood gene expression profiles in patients with venous thromboembolism

Xiaonan Chen, Jun Cao, Zi Ge, and Zhijie Xia

Emergency and Acute Critical Care Department, Huashan Hospital North, Fudan University, Shanghai, China

ABSTRACT

The main aim of this work was to evaluate differential expression and biological functions of circulating miRNA and whole peripheral blood (PB) genes in patients affected by venous thromboembolism (VTE) and in healthy subjects. Circulating miRNA sequences and PB expression profiles were obtained from GEO datasets. Ten miRNAs with the most significant differential expression rate (dif-miRNA) were subjected to miRbase to confirm their identity. Dif-miRNA targets were predicted by TargetScan and aligned with differentially expressed genes to obtain overlapping co-genes. Biological functions of co-genes were analyzed by Gene Ontology and KEGG analysis. Interaction network of dif-miRNAs, co-genes, and their downstream pathways were studied by analyzing protein–protein interaction (PPI) clusters (STRING) and determining the crucial hubs (Cytoscape).

MiR-522-3p and miR-134 dif-miRNAs are involved in protein translation and apoptosis by regulating their respective co-genes in PB. Co-genes are present in nucleolus and extracellular exosomes and are involved in oxidative phosphorylation and ribosome/poly(A)-RNA organization. The predicted PPI network covered 107 clustered genes and 220 marginal joints, where ten hub genes participating in PPIs were found. All these hub genes were down-regulated in VTE patients. Our study identifies new miRNAs as potential biological markers and therapeutic targets for VTE.

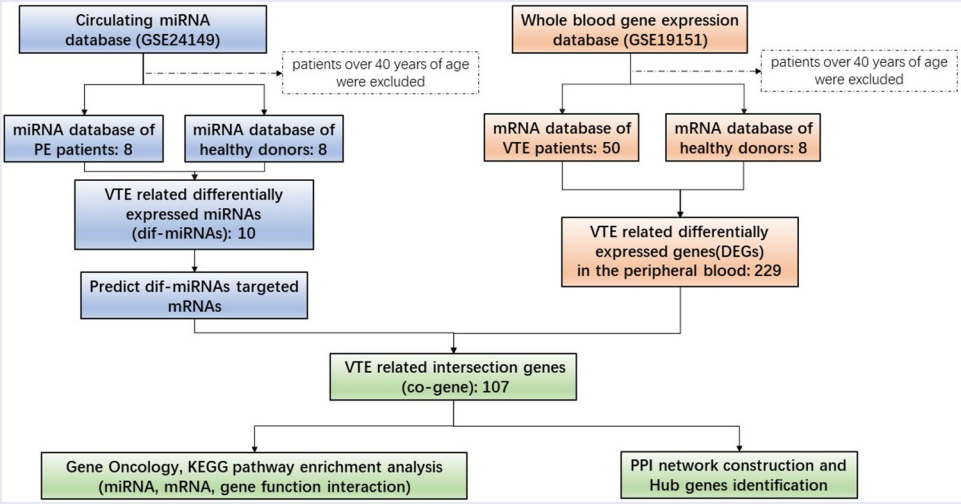

ARTICLE HISTORY
Received 19 March 2021
Revised 20 May 2021
Accepted 21 May 2021

KEYWORDS
Circulating microRNA; venous thromboembolism; biomarker candidates; genome-wide bioinformatic integration analysis

VTE, including deep vein thrombosis (DVT) and pulmonary embolism (PE), is the third most common acute and life-threatening cardiovascular condition, after myocardial infarction and stroke [1]. According to the epidemiological researches, the incidence rates of PE and DVT account for 0.39–1.15‰ and 0.53–1.62‰, respectively [2,3]. The annual mortality caused by PE in US reaches near 200,000, and most patients ultimately die within the first 1 h of PE presentation. In recent years, the diagnosed VTE cases have grown in China, with the proportion of PE patients rapidly increasing from 0.26‰ to 1.45‰ in 10 years [4,5]. Thus, early diagnosis and treatment of VTE can have great clinical relevance to reduce mortality.

CONTACT Zhijie Xia janexia_2006@126.com Emergency and Acute Critical Care Department, Huashan Hospital North, Fudan University

© 2021 The Author(s). Published by Informa UK Limited, trading as Taylor & Francis Group.
This is an Open Access article distributed under the terms of the Creative Commons Attribution-NonCommercial License (http://creativecommons.org/licenses/by-nc/4.0/), which permits unrestricted non-commercial use, distribution, and reproduction in any medium, provided the original work is properly cited.

MicroRNAs (miRNAs or miR) are highly conserved small non-coding RNA (containing about 22 nucleotides) that regulate gene expression by binding to the 3 -untranslated complementary region of target mRNAs and inducing their degradation or translation inhibition. Other than in cellular, miRNAs are also produced extracellular [6]. Recent evidence revealed different biological functions of circulating miRNAs, suggesting their possible role in the progresses of stroke, cardiovascular and metabolic diseases [7–10].

In order to unveil new biomarkers predisposing to VTE and potentially altered in high-risk population, the main goal of this study was to screen key circulating miRNAs related to the occurrence and progression of VTE disease and that were not identified by previous bioinformatics analyses. In this study, we analyzed new indicators of poor VTE prognosis and identified new potential therapeutic targets for this refractory disease. We compared differential whole blood gene expression in VTE patients and healthy donors, by using bioinformatic approaches and querying the Gene Expression Omnibus (GEO) datasets. We then associated biological functions to representative differentially expressed genes and enriched relevant signaling pathways by Kyoto Encyclopedia of Genes and Genomes (KEGG). We also established the protein–protein interaction networks to identify key hub genes and investigated related cellular biological process that may be regulated by circulating miRNAs. Based on the results, this study might provide new diagnostic tools for the prevention and early diagnosis of PTE.

Materials and methods

Microarray data

In order to evaluate the biological functions of circulating miRNAs in whole blood of VTE patients, we used expression data of circulating miRNA GSE24149 and whole blood gene expression GSE19151 from GEO database (https://www.ncbi.nlm.nih.gov/gds). GSE24149 was collected in 2010 in Shanghai, China. It contains plasma miRNA profiles from 10 PE patients and 10 healthy donors (age range: 20–82 years, no ethnic information available). GSE19151 dataset was collected in 2009 in Durham, USA. It contains gene expression profiles of plasma obtained from whole blood of 70 VTE patients and 63 control donors (age range: 18–84 years; 25 African Americans, 6 African Origin/Black, 95 Caucasians, 4 Hispanic or Latino, 1 Indian, 1 mixed, and 1 unclear ethnicity). Patients over 40 years of age were excluded from the study.

Identification of differentially expressed miRNAs and mRNAs relevant to VTE

The online bioinformatic tool GEO2 (http://www.ncbi.nlm.nih.gov/geo/geo2r/) was used to compare multiple GEO lists and recognize significant expression differences. The automatic algorithm of GEO2R is designed to calibrate p values with false discovery rate (FDR) correction when performing multiple t-test analysis. Here, we utilized GEO2R to extract the differential expression lists. The differentially expressed genes were defined with the significance of $|\log FC| > 1$ and $p < 0.05$.

Acquisition of VTE-related gene list

miRbase (http://mirbase.org/index.shtml) is a primary open repository which archives published miRNA sequences and annotation and provides target gene prediction service. The latest version is 22.

TargetScan (http://www.targetscan.org/vert_72/) is an online software, widely used for prediction of miRNA binding sites on target genes. It can search conserved 8-mer, 7-mer and 6-mer sites that are compatible with miRNA seed regions. We searched for the 10 most differentially upregulated or downregulated miRNAs (dif-miRNA) into miRbase to confirm their identities, followed by target gene prediction with TargetScan. We then compared these predicted target genes with GSE19151 list to obtain an intersection list (co-gene).

GO and KEGG analysis of miRNA target genes

GO is bioinformatic analysis widely used to enrich and assign genes to pre-defined functional characteristics comprising biological process, cellular components, and molecular function. Also, KEGG database is an extensively used database,

storing plentiful resources of genome, biological pathways, diseases and data related to chemical substances and drugs. In this study, we analyzed DEG with GO annotations and KEGG pathway enrichment on Database for Annotation, Visualization and Integrated Discovery (DAVID): https://david.ncifcrf.gov/. P <0.05 and gene count ≥ 5 were considered statistically significant.

PPI establishment and hub gene identification

The STRING database (http://string-db.org/) provides information on the protein–protein interaction (PPI). In order to analyze the PPI of co-genes, we mapped co-gene interaction network through STRING database and extracted PPI pairs based on a combination score >0.4. Subsequently, the PPI network was visualized through Cytoscape (www.cytoscape.org/). The tendency of PPI was evaluated by the Cytoscape plug-in CytoHubba. Gene nodes with multiple interactive connections were crucial in maintaining the stability of the entire network. In our research, the top-ten nodes with the most active connectivity were identified as Hub genes.

Results

Differentially expressed circulating miRNAs and peripheral blood whole blood genes (DEG)

In order to unveil differentially expressed circulating miRNAs and differentially expressed genes (DEG) in whole peripheral blood, we compared the expression profiles of VTE patients and control group in the two datasets analyzed.

From the analysis of GSE24149 dataset of circulating miRNA, 220 and 12 circulating miRNAs were found to be upregulated and downregulated, respectively, in PE patients, as compared to healthy control groups. Among the differentially expressed miRNAs, ten dif-miRNAs with the higher |LogFC| value were further analyzed (Table 1). In parallel, from the analysis of GSE19151 dataset of whole blood gene expression profile, among the 229 DEGs in the peripheral blood of VTE patients, 2 were up-regulated and 227 were down-regulated (Table 2).

Table 1. Top ten miRNAs with the most significant differential expressions in peripheral blood of VTE patients.

miRNA ID	Adjusted ID	LogFC	P Value
hsa-miR-144*	hsa-miR-144-5p	−3.49593	0.0301
hsa-let-7 g	hsa-let-7 g-5p	−3.30413	0.0122
hsa-miR-20a*	hsa-miR-20a-3p	−3.08215	0.0144
hsa-miR-7	hsa-miR-7-5p	−2.95788	0.0144
hsa-miR-942	hsa-miR-942	−2.79764	0.0301
hsa-miR-874	hsa-miR-874	5.18195	0.0121
hsa-miR-522	hsa-miR-522-3p	5.07948	0.0476
hsa-miR-193a	hsa-miR-193a	3.62387	0.0121
hsa-miR-134	hsa-miR-134	3.56239	0.0121
hsa-miR-483	hsa-miR-483-3p	3.2528	0.0121

Detection and functional enrichment analysis of co-genes in VTE patients

We used TargetScan to detect target mRNAs of the circulating dif-miRNAs. DEG of GSE19151 were compared with common DEGs and named co-genes (Table 3, Figure 1). We then focused on the 107 co-genes and investigated their biological function by using the DAVID online bioinformatic tool for GO enrichment and KEGG pathway analysis.

GO enrichment analysis covers three fields, including biological processes, cellular component, and molecular function. The results of GO analysis suggested that the identified co-genes were involved in translation and negative regulation of apoptosis. These processes were, next, related to dif-mRNA and co-genes by constructing a miRNA-gene-biological process interaction network (Figure 2). The network map showed that 11 co-genes participated in the two biological processes and 5 dif-miRNAs played a pivotal regulatory role. Co-genes were associated with cellular components, including nucleolus and extracellular exosomes. MF analysis implied that co-genes were actively involved in structural constituents of ribosomes and poly-(A) RNA binding activity (Table 4). In addition, the results of KEGG pathway analysis showed that co-genes were mainly present in pathways related to ribosomes, oxidative phosphorylation, as well as in Parkinson's disease, nonalcoholic

Table 2. Differentially expressed genes (DEGs) in peripheral blood of VTE patients.

Gene.symbol	P Value	logFC	Gene.symbol	P Value	logFC	Gene.symbol	P Value	logFC
TLN1	0.002311	1.052952	HSP90AA1	0.002017	−1.80932	RPL31	0.005412	−1.92844
ZFP36L1	0.005728	1.152931	HSPE1-MOB4	0.012055	−1.34059	RPL34	0.009949	−1.4919
ACADM	0.011272	−1.08054	IFIT1	0.004666	−2.16111	RPL36A	0.015296	−1.58538
ACTR6	0.01149	−1.25503	IFIT5	0.005731	−1.10699	RPL36AL	0.001992	−1.25677
AGL	0.01416	−1.58293	IL6ST	0.015079	−1.04166	RPL39	0.006067	−1.33649
AK6	0.005524	−1.13278	IMPA1	0.014093	−1.28687	RPL41	0.006066	−1.03092
AKR1C3	0.005214	−1.33393	ITGAV	0.011772	−1.05021	RPL7	0.004045	−1.70641
ANKRD49	0.013643	−1.06019	JAK2	0.012256	−1.19741	RPL9	0.002887	−1.87196
ANP32E	0.013272	−1.39025	KIAA0391	0.002086	−1.61566	RPS15A	0.005669	−1.15386
ANXA1	0.003366	−1.53284	KLRB1	0.005296	−1.3837	RPS17	0.004258	−1.45516
ANXA3	0.014972	−1.25051	KLRF1	0.011312	−1.19703	RPS23	0.002284	−1.69922
ATAD2B	0.013658	−1.13958	KTN1	0.003373	−1.50054	RPS24	0.005425	−1.65096
ATG5	0.011539	−1.00773	LAMTOR3	0.014781	−1.29482	RPS27A	0.002842	−1.01885
ATP5C1	0.002023	−1.54041	LPAR6	0.001768	−1.71736	RPS27L	0.003608	−1.68584
ATP5F1	0.002086	−1.37046	LRRC40	0.013329	−1.16338	RPS7	0.003344	−2.08102
ATP5O	0.003169	−1.29712	LSM5	0.002711	−1.43599	RSL24D1	0.011772	−1.62669
ATP6V1C1	0.002693	−1.11276	LY96	0.011837	−1.15484	RWDD1	0.003345	−1.27051
ATP6V1D	0.001203	−1.1632	MBNL1	0.004213	−1.16926	SAMD9	0.00434	−1.18383
BCL2A1	0.010465	−1.7155	MBNL2	0.009319	−1.01842	SAR1B	0.003997	−1.15723
BIRC2	0.011542	−1.42805	MCTS1	0.001768	−1.3979	SEC62	0.012933	−1.152
C12orf29	0.005296	−1.21351	MDH1	0.001845	−1.19747	SH2D1A	0.004369	−1.34456
C14orf2	0.007742	−1.05559	MED21	0.001385	−1.34853	SKIV2L2	0.007982	−1.10264
C4orf46	0.009319	−1.36502	MRPL13	0.007877	−1.03596	SLC30A1	0.01449	−1.07211
CAPZA1	0.005565	−1.04274	MRPL15	0.001992	−1.14411	SMC4	0.012048	−1.323
CAPZA2	0.007171	−1.43103	MRPL3	0.003416	−1.46333	SNHG4	0.002842	−1.45734
CASP3	0.003645	−1.22233	MRPL42	0.003911	−1.20088	SNORA21	0.00596	−1.58185
CCDC91	0.006256	−1.24315	MS4A4A	0.007398	−1.36585	SNORD54	0.001992	−1.04649
CCNC	0.014805	−1.19752	MTHFD2	0.002228	−1.43667	SNORD73A	0.001992	−2.51606
CCT2	0.001768	−1.30835	MYBL1	0.00434	−1.55335	SNRPD2	0.002749	−1.51699
CD2AP	0.014103	−1.1228	MYL6	0.002056	−1.02559	SNRPG	0.01334	−1.2511
CD69	0.009904	−1.25466	NAA15	0.007877	−1.12972	SNX4	0.003147	−1.25499
CD86	0.001203	−1.17836	NAB1	0.011071	−1.08198	SRP19	0.002783	−1.09312
CEBPZ	0.002086	−1.38956	NAT1	0.007982	−1.03158	SRP72	0.001203	−1.14042
CEP57	0.003416	−1.18991	NDUFA1	0.002991	−1.1217	SSB	0.002086	−1.08434
CHD9	0.00717	−1.08933	NDUFA4	0.004017	−1.52358	STAG2	0.007282	−1.14388
CHMP5	0.007982	−1.1441	NDUFA5	0.015165	−1.42653	STX7	0.008636	−1.06838
CKS2	0.002887	−1.30107	NDUFA6	0.00251	−1.03084	SUB1	0.006428	−1.59265
CLEC2B	0.011826	−1.34674	NDUFB2	0.002603	−1.07679	SUCLA2	0.007537	−1.2347
CLEC4A	0.007489	−1.02954	NOC3L	0.002559	−1.35069	SUZ12	0.003601	−1.05487
CNIH4	0.010066	−1.14621	NRG1	0.010622	−1.09154	SYNCRIP	0.014028	−1.17322
COMMD8	0.007995	−1.55772	NSA2	0.003472	−1.06913	TAF7	0.007732	−1.14536
COPS2	0.002136	−2.01753	NUCB2	0.007942	−1.08371	TAX1BP1	0.002693	−1.06852
COPS4	0.001768	−1.43139	NUP58	0.009068	−1.06209	TBC1D15	0.006449	−1.1647
COX7A2	0.010036	−1.07453	NXT2	0.004281	−1.2521	TFEC	0.008791	−1.42258
COX7C	0.01057	−1.16601	OXR1	0.006095	−1.50406	THAP12	0.014428	−1.07614
CSNK1G3	0.011542	−1.01867	PDCD10	0.005711	−1.50133	TMCO1	0.002086	−1.5828
CSTA	0.007942	−1.73005	PEX2	0.003428	−1.2965	TMEM126B	0.007907	−1.20502
CYCS	0.009109	−1.0075	PFDN5	0.005586	−1.41994	TMEM135	0.010003	−1.11086
CYP1B1	0.011708	−1.11298	PHIP	0.010089	−1.3841	TMF1	0.009224	−1.07832
DBI	0.01023	−1.30864	PIGK	0.002056	−1.37603	TMX1	0.004423	−1.38867
DCUN1D1	0.01051	−1.25808	PIK3R1	0.002336	−1.03532	TNFAIP6	0.015404	−1.36049
DDX50	0.002056	−1.12659	PMAIP1	0.007907	−1.09809	TNFSF10	0.002082	−1.0818
DDX60	0.014028	−1.05148	PNRC2	0.009011	−1.07693	TRAT1	0.004006	−1.52595
DNAJA1	0.002647	−1.2838	POLR2K	0.009028	−1.13872	TRIM23	0.006705	−1.24923
DNAJC15	0.003366	−1.23698	POT1	0.005214	−1.03065	TTC33	0.010622	−1.07746
DPM1	0.009109	−1.14624	PPA2	0.001203	−1.26725	TWF1	0.012556	−1.19069
DYNLT3	0.003366	−1.48072	PPIG	0.003428	−1.09525	TXNDC9	0.003068	−1.4978
EIF3E	0.001992	−1.85498	PRKACB	0.002209	−1.44721	UCHL3	0.002306	−1.044
EMC2	0.014656	−1.0368	PRPF18	0.009109	−1.00778	UFL1	0.002284	−1.19304
ERGIC2	0.007784	−1.02373	PSMA2	0.002412	−1.60226	UQCRB	0.015198	−1.24802
EVI2A	0.002664	−2.28923	PSMA3	0.003815	−1.07933	UQCRH	0.001768	−1.36602
FAM35A	0.009392	−1.30097	PSMA4	0.004258	−1.45532	UQCRQ	0.004213	−1.58026
FPGT	0.014181	−1.06812	PSMC6	0.006492	−1.78049	USP1	0.002136	−1.13526
GALNT1	0.00292	−1.02446	PSMD10	0.007084	−1.0229	USP16	0.006337	−1.11092

(*Continued*)

Table 2. (Continued).

Gene.symbol	P Value	logFC	Gene.symbol	P Value	logFC	Gene.symbol	P Value	logFC
GLRX	0.00396	−1.25846	PTP4A1	0.007236	−1.0124	VAMP7	0.001992	−1.28107
GMFB	0.010692	−1.10799	PTPN4	0.001629	−1.07738	ZBED5	0.006728	−1.21001
GNAI3	0.002965	−1.05599	PYROXD1	0.005212	−1.3728	ZC3H15	0.001992	−1.18085
GPR65	0.004174	−1.6033	RB1CC1	0.003366	−1.49063	ZCCHC10	0.011199	−1.30082
GTF2B	0.002693	−1.21	RBM39	0.015482	−1.0927	ZNF22	0.002782	−1.20885
GTF2H5	0.002694	−1.2895	RCN2	0.002653	−1.21558	ZNF267	0.006492	−1.57868
GZMA	0.007687	−1.12829	RDX	0.006646	−1.01147	ZNF292	0.003997	−1.44021
HAT1	0.004271	−1.79111	RPA3	0.002693	−1.14171	ZNF654	0.012597	−1.11143
HINT1	0.005014	−1.32867	RPAP3	0.010622	−1.05527	ZNF83	0.01493	−1.20098
HLTF	0.005211	−1.17621	RPL10	0.003134	−1.17675	ZNHIT3	0.003453	−1.20255
HMGB1	0.002744	−1.06703	RPL17	0.0049	−1.73562	ZZZ3	0.010504	−1.08037
HNMT	0.008262	−1.22766	RPL21	0.007635	−1.24714			
HPR	0.011008	−1.01855	RPL27	0.002086	−1.13051			

Table 3. Overlapping gene list (co-genes) of dif-miRNAs target genes and DEGs in VTE patients.

Dif-miRNAs	Co-genes
hsa-miR-20a-3p	TLN1
hsa-miR-874	IMPA1, TTC33, NDUFA5, RPS23, TRAT1, RPAP3, STX7, MBNL1, TMF1, HNMT, RPS24, PMAIP1, HAT1, SEC62, TNFSF10, RPS27A, IFIT1, TMCO1
hsa-miR-522-3p	ATP5F1, DNAJC15, ANKRD49, UFL1, ATP6V1C1, RDX, GTF2H5, UQCRQ, PTPN4, RB1CC1, DPM1, MRPL13, RPL9, NAB1, IMPA1, PIK3R1, TMEM135, VAMP7, TTC33, HINT1, NDUFA5, HMGB1, MBNL2, GNAI3, SH2D1A, ATAD2B, CHMP5, TRAT1, RPAP3, STX7, OXR1, CASP3, PEX2, CAPZA1, MRPL3, LSM5, RPS15A, DCUN1D1, MBNL1, LRRC40, IL6ST, TXNDC9, TMX1, PTP4A1, SAMD9, CEP57, TMF1, CYCS, EVI2A, NOC3L, PYROXD1, COMMD8, MYBL1, EMC2, MS4A4A, SYNCRIP, CCDC91, SUZ12, RPA3, PPA2, RBM39, NXT2, COX7C, ZC3H15, RSL24D1, CAPZA2, RPS27A, PPIG, SMC4, C12orf29, ATG5, DNAJA1, CCNC, ZNF292, PSMA4, MCTS1, PHIP, PNRC2, RWDD1, TMCO1, ZNF654, ATP6V1D, ZZZ3, NRG1
hsa-miR-193a	ATP5F1, MRPL3, GMFB, NRG1, CEP57
hsa-miR-134	ATP5F1, ANKRD49, ATP6V1C1, RDX, LAMTOR3, PTPN4, NAB1, TBC1D15, PIK3R1, TMEM135, RCN2, NDUFA5, HMGB1, SH2D1A, ATAD2B, NDUFA4, CAPZA1, MRPL3, POLR2K, RPS15A, DCUN1D1, MBNL1, LRRC40, IL6ST, SAMD9, CEP57, TMF1, SAR1B, CYCS, HNMT, RPS24, CD86, GTF2B, CNIH4, GLRX, SEC62, GALNT1, CAPZA2, PPIG, MTHFD2, ATG5, PSMA4, FAM35A, IFIT1, RWDD1, NRG1
hsa-miR-483-3p	UQCRQ, NRG1, RPS24, ZNF292

fatty liver disease (NAFLD), Huntington's and Alzheimer's disease (Table 5).

PPI network construction and Hub genes identification

In order to clarify the interaction network between the downstream proteins of co-genes and explore the core regulatory genes, STRING was used to predict the interaction of 107 co-genes at protein level.

As shown in Figure 3, a total of 107 gene nodes and 220 marginalized genes are present in PPI network. We further identified the top-ten Hub genes evaluated by connectivity in the PPI network (Table 6). Among them, we found a high connectivity for ribosomal protein S27a (RPS27A) (score = 24), together with cytochrome c, somatic (CYCS; score = 17), mitochondrial ribosomal protein L13 (MRPL13; score = 16), ribosomal protein L9, ribosomal protein S15a (RPL9, RPS15A; score = 15), ribosomal protein S24 (RPS24; score = 14), ribosomal protein S23 and proteasome 20S subunit alpha 4 (RPS23, PSMA4; score = 13), histidine triad nucleotide binding protein 1 and for NDUFA4 mitochondrial complex associated (HINT1, NDUFA4; score = 12). All these hub genes were down-regulated in VTE patients.

Finally, we established an interaction network among dif-miRNA, Hub gene, and KEGG pathway (Figure 4).

Discussion

VTE is a common peripheral vascular disease (PVD). Thrombus shedding in acute stage of VTE may cause fatal pulmonary embolism, which is one of the primary causes of sudden clinical death. Recent studies showed that PE and DVT are frequent clinical manifestations of VTE. Deep

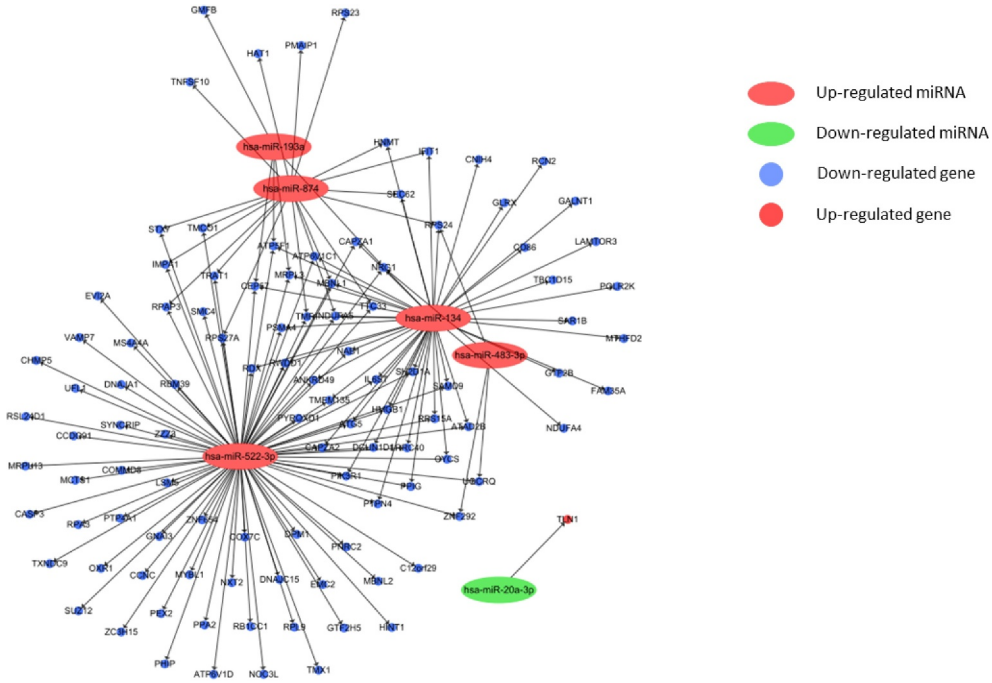

Figure 1. Interaction network of dif-miRNAs and their co-gene targets in VTE patients.

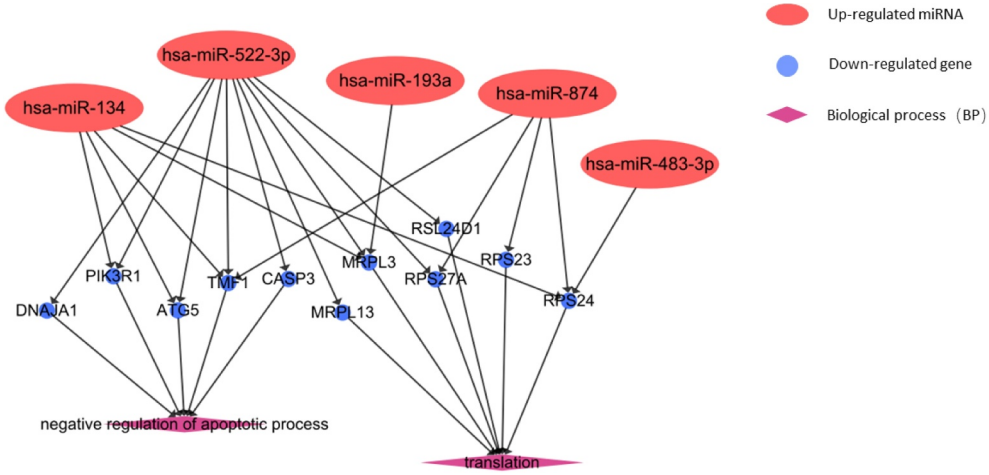

Figure 2. Predicted regulation on biological process (BP) of Co-genes by Dif-miRNAs in VTE patients.

vein thrombosis and pulmonary embolism are manifestations of venous thromboembolism at different stages, especially in patients with lower extremity DVT. Current case reports showed that deep vein thrombosis as well as pulmonary embolism are the most preventable causes of death in hospital [11]. Early detection, diagnosis and treatment are clinically important to reduce the VTE fatality. Although the D-dimer evaluation, color Doppler blood flow imaging, venography and other approaches have increased the sensitivity and specificity of VTE diagnosis, there is still an urgent need for better, alternative diagnostic methods, also due to nonspecific symptoms of VTE and the restriction of current detective approaches.

Although miRNAs are mainly present in cells, they can be released extracellularly through the exosome secretion pathway. Circulating miRNA are involved in intercellular communications, in biological functional regulation, as well as can promote disease progression [12–15]. Moreover, research showed that circulating miRNAs regulate gene expression through its impact on mRNA

Table 4. Gene ontology (GO) function enrichment analysis of co-genes in VTE patients.

Category	Term	P Value	Count	Genes
BP	translation	0.005175078	6	MRPL13, MRPL3, RSL24D1, RPS27A, RPS23, RPS24
BP	negative regulation of apoptotic process	0.04424408	5	CASP3, ATG5, DNAJA1, PIK3R1, TMF1
CC	nucleolus	1.15E-04	13	TMX1, ZC3H15, NOC3L, GTF2H5, GTF2B, SUZ12, RPL9, ZZZ3, RSL24D1, RPS23, RPS27A, RCN2, OXR1
CC	extracellular exosome	0.01487892	22	TLN1, LAMTOR3, STX7, IMPA1, GNAI3, CHMP5, IL6ST, CAPZA2, RDX, ATP6V1D, PPA2, PHIP, ATP6V1C1, TBC1D15, CD86, TNFSF10, HNMT, PTP4A1, VAMP7, DNAJA1, RPS27A, GLRX
MF	structural constituent of ribosome	9.78E-04	7	MRPL13, MRPL3, RPL9, RSL24D1, RPS27A, RPS23, RPS24
MF	poly(A) RNA binding	0.006437021	12	HMGB1, MRPL3, PPIG, ZC3H15, NOC3L, SYNCRIP, MBNL2, RDX, MBNL1, RBM39, RPS27A, RPS23

Abbreviation:BP, biological process; CC, cellular component; MF, molecular function.

Table 5. KEGG enrichment analysis of in VTE patients.

Category	Term	P Value	Count	Genes
KEGG_PATHWAY	cfa03010:Ribosome	9.17E-05	8	MRPL13, MRPL3, RPL9, RPS15A, RSL24D1, RPS27A, RPS23, RPS24
KEGG_PATHWAY	cfa00190:Oxidative phosphorylation	0.003555	6	ATP6V1C1, NDUFA4, NDUFA5, UQCRQ, ATP6V1D, PPA2
KEGG_PATHWAY	cfa05012:Parkinson's disease	0.004271	6	NDUFA4, NDUFA5, CASP3, GNAI3, CYCS, UQCRQ
KEGG_PATHWAY	cfa04932:nonalcoholic fatty liver disease (NAFLD)	0.004943	6	NDUFA4, NDUFA5, CASP3, CYCS, UQCRQ, PIK3R1
KEGG_PATHWAY	cfa05016:Huntington's disease	0.014098	6	NDUFA4, NDUFA5, CASP3, POLR2K, CYCS, UQCRQ
KEGG_PATHWAY	cfa05010:Alzheimer's disease	0.03951	5	NDUFA4, NDUFA5, CASP3, CYCS, UQCRQ

transcription [16,17]. Our results demonstrated that several circulating miRNAs can take active part in post-transcriptional modifications and mRNA stabilization through regulating nuclear genes and participating in poly(A) RNA binding processes (Table 4). Nowadays, the measurement of circulating miRNAs as VTE diagnostic approach is drawing great attention. Compared to conventional protein biomarkers, circulating miRNA has many advantages, including: ① the stability of circulating miRNA makes the detection reproducible; ② the variabilities of circulating miRNA expression are specifically related to the disease; ③ sample collection for circulating miRNAs is less invasive, more convenient for detection and analysis; ④the increase of circulating miRNA level can be considered as an early signal of disease, compared to protein biomarkers.

In this study, circulating miRNA and gene expression analyses were performed with the GEO database. We analyzed circulating miRNAs and genes differentially expressed in the peripheral whole blood of VTE patients and healthy donors. GSE24149 contains only data relative to 4 subjects under 40. The mean age ± standard deviation was 49 ± 18.31 years, the median was 50 years, the 25% and 75% percentiles were 42.25 and 59.5 years, respectively. However, 73 out of 133 samples of GSE19151 came from subjects under 40 and 2 from subjects with unknown age. The mean age ± standard deviation was 39.85 ± 17.66 years, the median was 36 years, the 25% and 75% percentiles were 25 and 50 years, respectively. Considering that differences in age distribution could affect analysis results, patients over 40 years were excluded from the study. Data adjustment reduced differences in age distribution of the two datasets, and further analysis of the datasets showed that the mean age distribution ± standard deviation in GSE24149 (16 samples) was 56.13 ± 12.40 years, the median was 52 years, the 25% and 75% percentiles were 47 and 67.75 years, respectively. After adjustment, the mean of age distribution ± standard deviation in GSE19151 (58 samples) was 56.33 ± 12.98 years, the median was 52.00 years, the 25% and 75% percentiles were 45 and 68.50 years, respectively (Figure 5). We identified one up-regulated and 106 down-regulated co-genes and constructed a PPI network to further identify the relationships between these dif-

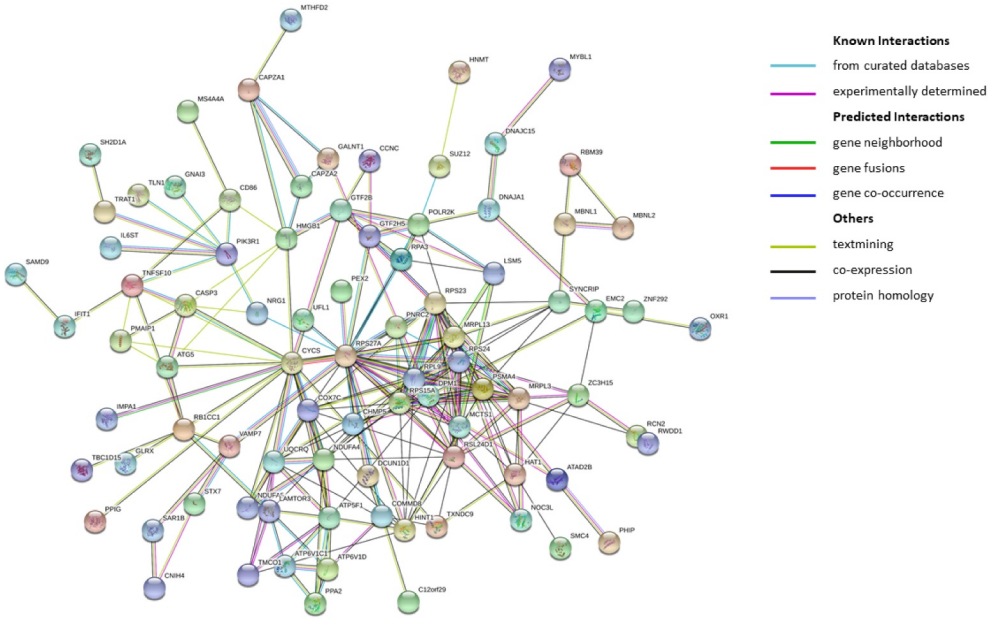

Figure 3. STRING protein–protein interaction analysis of co-genes.

Table 6. Top ten co-genes genes (hub genes) with highest connectivities.

Rank	Name	Score	Description
1	RPS27A	24	ribosomal protein S27a
2	CYCS	17	cytochrome c, somatic
3	MRPL13	16	mitochondrial ribosomal protein L13
4	RPL9	15	ribosomal protein L9
4	RPS15A	15	ribosomal protein S15a
6	RPS24	14	ribosomal protein S24
7	RPS23	13	ribosomal protein S23
7	PSMA4	13	proteasome 20S subunit alpha 4
9	HINT1	12	histidine triad nucleotide binding protein 1
9	NDUFA4	12	NDUFA4 mitochondrial complex associated

miRNAs and co-genes. We then focused on 10 critical hub genes presumably targeted by dif-miRNAs. Our study on VTE-related miRNA regulation proposes a novel methodological approach for early VTE diagnosis.

According to the traditional view, venous thrombosis is related to red blood cells, producing 'red thrombus' rich in fibrin, whereas arterial thrombus is rich in platelets, forming 'white thrombus.' However, current experimental studies have shown that platelet activation is also involved in venous thrombosis [18]. Platelets can be used not only as a donor of miRNA but also as a recipient of circulating miRNA. In recent years, studies have found that miRNAs can be combined with the mRNA of multiple key factors in the coagulation-anticoagulation and fibrinolysis

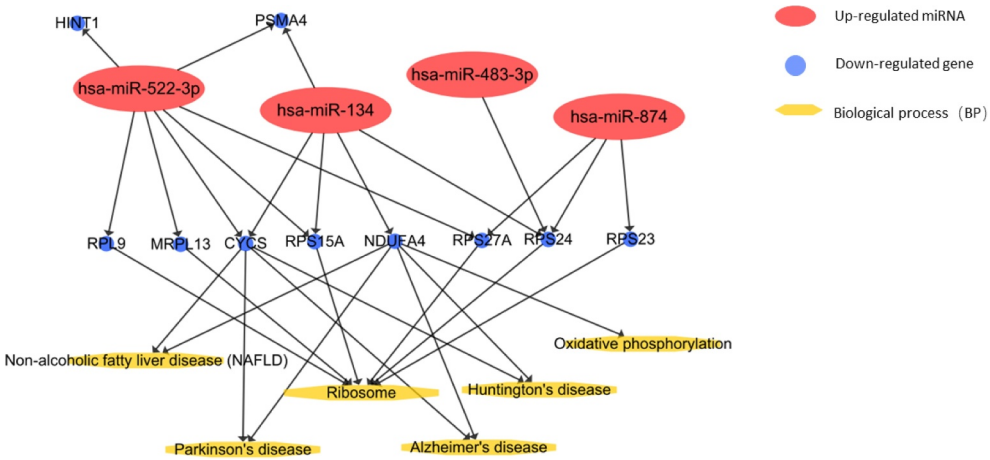

Figure 4. Predicted KEGG pathways involving top 10 hub genes regulated by dif-miRNAs in peripheral blood of VTE patients.

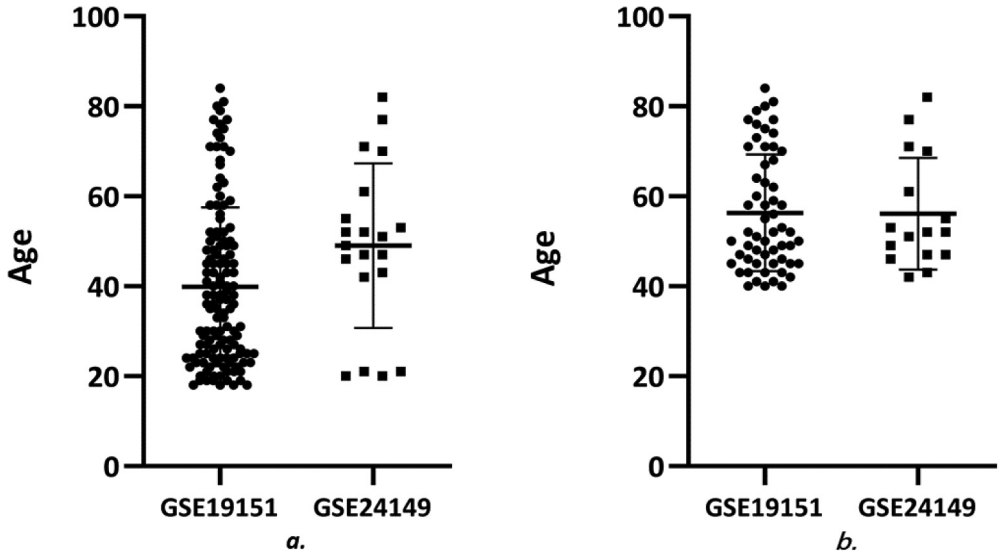

Figure 5. Age distribution in each dataset before and after preprocessing (a. before preprocessing b. after preprocessing).

system and regulate the process of thrombosis and dissolution at gene level. For example, miR-223, miR-96, miR-200b, etc. can inhibit platelet protein expression through miRNA-mRNA pathway, thereby affecting platelet function. miR-494, miR-27a, miR-27b can be combined with the 3 UTR of tissue factor pathway inhibitor (TFPI) mRNA and promote thrombosis by down-regulating the expression of TFPIα [19]. Studies have shown that there is a certain amount of ribosomal protein in platelets [20]. For example, ribosomal protein S6K1 and SLFN14 are present in circulating platelets and exert their unique effects in the process of hemostasis and thrombosis [21,22]. The polymorphism of ribosomal protein MRPL37 predisposes to recurrent venous thromboembolism [23]. In our study, the Hub genes RPS27A, MRPL13, RPL9, RPS23, and RPS24 belong to the ribosomal protein family. We observed circulating hsa-miR -522-3p, -134, -874, -483 – through KEGG pathway analysis. miR-522-3p participates in the metabolic process of ribosomal protein family by regulating the aforementioned Hub genes. At present, few reports on the relationship between these miRNA-ribosomal protein family genes and venous thrombosis are available. Therefore, we speculate that the identified miRNA-genes may be closely related to platelet activation and may be new potential markers.

Vascular endothelial cells play an important role in the process of thrombosis. After endothelial cells are destroyed, collagen and intravascular tissue factors are exposed to the bloodstream, with thrombus beginning to form. The exposed collagen triggers the activation and accumulation of platelets, whereas tissue factors trigger the production of thrombin that converts fibrinogen into fibrin and activates platelets. Therefore, endothelial dysfunction can be considered as a risk factor for thrombosis. In recent years, a number of studies have suggested that miR-31, miR-20a, and miR-29b can regulate the expression level of TNFSF15–TNFRSF25 through related cell pathways [24–26], and the pathological up-regulation of TNFSF15–TNFRSF25 can lead to the occurrence and progression of primary venous thromboembolism by exerting its pro-apoptotic and anti-proliferative activities on endothelial cells [27]. In vitro studies have also demonstrated that miR-134 can aggravate glucose-induced endothelial cell dysfunction, whereas miR-874-3p can antagonize the damage of high glucose to endothelial cells [28,29]. Our research shows that circulating hsa-miR-134, -522-3p and -874 are involved in the inhibition of apoptotic processes during the progression of VTE by regulating CASP3, ATG5, DNAJA1, PIK3R1, and TMF1 genes. The latter can in turn regulate the apoptosis of vascular endothelial cells in VTE.

Exosomes can promote the exchange of peptides, miRNAs, mRNA and mitochondrial DNA between cells and tissues. They play an important role in

many physiological and pathological processes and can be used as diagnostic markers for various cardiovascular diseases [30]. Vascular endothelial cells and platelets can produce a large number of exosomes. The apoptotic bodies, MVs and exosomes released by caspase-3-activated VECs were analyzed by large-scale proteomics. Protein expression profiles of the body showed that the 20S proteasome activity in circulating exosome-like vesicles increased after vascular injury in mice [31]. Platelet-derived exosomes are rich in a variety of miRNAs with regulatory functions. Among them, the levels of miR-223, miR-339 and miR-21 are related to platelet activation, with miR-223 being the most abundant miRNA in platelets and contributing to platelet activation, reactive secretion, adhesion and aggregation [32]. These exosomal miRNAs can be used as biomarkers to predict thrombosis [33]. Antiplatelet therapy can significantly reduce the levels of these miRNAs. Similarly, we suggest that circulating miR-20a- 3p, -134, -522-3p, and -874 can regulate the expression of genes encoding components of exosomes, including TLN1, LAMTOR3, STX7, and IMPA1, thus controlling the involvement of exosomes in the pathophysiological activities associated to VTE.

Although we found new targets with potential research value, our research has some limitations. The analyzed datasets are all taken from the GEO library. Thus, considering the differences in datasets on the aspects of experimental conditions and candidates' ethnicity and living environment, there are limitations in further clarifying the association between miRNA-gene and disease. Future experiments verifying the relevance of these miRNA-mRNA pairs in specific populations, as well as tests in animal models are needed. Secondly, in addition to peripheral whole blood, miRNAs may also be enriched in other potential target tissues, such as endothelium of diseased blood vessels and thrombus components.

Conclusion

In this study, we showed a comprehensive analysis of the entire genome of VTE patients performed by analyzing their circulating miRNA and gene interactions. We also described the relationship between several miRNA-based circulating biomarkers and key genes in peripheral whole blood. Our findings explained the biological functions of these blood biomarkers in VTE patients, thus providing new targets with strong research value.

Highlights

1. Some new miRNAs and hub genes as potential biological markers and therapeutic targets for VTE were identified.
2. We identify new gene regulation mechanisms involved in the progression of VTE.
3. We provide new useful tools to identify those individuals potentially subjected to VTE.

Disclosure of conflict of interest

The authors declared that they do not have any commercial or associative interest that represents a conflict of interest in connection with the work submitted.

Funding

This work was supported by Special Project of Shanghai Municipal Economic and Information Technology Commission [Project No 201601028], Key Medical Project of Science and Technology Support Plan of Shanghai Science and Technology Commission [Project No 1641 1954400], General Project of Shanghai Municipal Health and Family Planning Commission [Project No 201640181].

ORCID

Zhijie Xia http://orcid.org/0000-0002-3854-9803

References

[1] Raskob GE, Angchaisuksiri P, Blanco AN, et al. Thrombosis: a major contributor to global disease burden[J]. Arterioscler Thromb Vasc Biol. 2014;34 (11):2363–2371.
[2] Wendelboe AM, Raskob GE. Global burden of thrombosis: epidemiologic aspects[J]. Circ Res. 2016;118 (9):1340–1347.
[3] Keller K, Hobohm L, Ebner M, et al. Trends in thrombolytic treatment and outcomes of acute pulmonary embolism in Germany. Eur Heart J. 2020;41 (4):522–529.
[4] Fesmire FM, Brown MD, Espinosa JA, et al. Critical issues in the evaluation and management of adult patients presenting to the emergency department with suspected pulmonary embolism. Ann Emerg Med. 2011;57(6):628–652.

[5] Xu XF, Yang YH, Zhai ZG, et al. Prevalence and incidence of deep venous thrombosis among patients in medical intensive care unit. Zhonghua Liu Xing Bing Xue Za Zhi. 2008;29(10):1034–1037.
[6] Zampetaki A, Willeit P, Drozdov I, et al. Profiling of circulating microRNAs: from single biomarkers to re-wired networks. Cardiovasc Res. 2012;93(4):555–562.
[7] Kumar S, Williams D, Sur S, et al. Role of flow-sensitive microRNAs and long noncoding RNAs in vascular dysfunction and atherosclerosis. Vasc Pharmacol. 2019;114:76–92.
[8] Ultimo S, Zauli G, Martelli AM, et al. Cardiovascular disease-related miRNAs expression: potential role as biomarkers and effects of training exercise. Oncotarget. 2018;9(24):17238–17254.
[9] Barutta F, Bellini S, Mastrocola R, et al. MicroRNA and microvascular complications of diabetes. Int J Endocrinol. 2018;2018:6890501.
[10] Dewdney B, Trollope A, Moxon J, et al. Circulating MicroRNAs as biomarkers for acute ischemic stroke: a systematic review. J Stroke Cerebrovasc Dis. 2018;27(3):522–530.
[11] Michota FA. Bridging the gap between evidence and practice in venous thromboembolism prophylaxis: the quality improvement process. J Gen Intern Med. 2007;22(12):1762–1770.
[12] Xu H, Du X, Xu J, et al. Pancreatic β cell microRNA-26a alleviates type 2 diabetes by improving peripheral insulin sensitivity and preserving β cell function. PLoS Biol. 2020;18(2):e3000603.
[13] Wang S, Min J, Yu Y, et al. Differentially expressed miRNAs in circulating exosomes between atrial fibrillation and sinus rhythm. J Thorac Dis. 2019;11(10):4337–4348.
[14] Patil M, Henderson J, Luong H, et al. The art of intercellular wireless communications: exosomes in heart disease and therapy. Front Cell Dev Biol. 2019;7:315.
[15] Sundar IK, Li D, Small RI. RNA-sequence analysis of plasma-derived extracellular vesicle miRNAs in smokers and patients with chronic obstructive pulmonary disease as circulating biomarkers. J Extracell Vesicles. 2019;8(1):1684816.
[16] Chen J, Tian J, Tang X, et al. MiR-346 regulates CD4 CXCR5 T cells in the pathogenesis of Graves' disease. Endocrine. 2015;49(3):752–760.
[17] Rodríguez-Muñoz A, Martínez-Hernández R, Ramos-Leví AM, et al. Circulating microvesicles regulate Treg and Th17 differentiation in human autoimmune thyroid disorders. J Clin Endocrinol Metab. 2015;100(12):E1531–E1539.
[18] Jerjes-Sánchez C, Villarreal-Umaña S, Ramírez-Rivera A, et al. Improving adjunctive treatment in pulmonary embolism and fibrinolytic therapy. The role of enoxaparin and weight-adjusted unfractionated heparin. J Thromb Thrombolysis. 2009;27(2):154–162.
[19] Ali HO, Arroyo AB, González-Conejero R, et al. The role of microRNA-27a/b and microRNA-494 in estrogen-mediated downregulation of tissue factor pathway inhibitor α. J Thromb Haemost. 2016;14(6):1226–1237.
[20] Mills EW, Wangen J, Green R, et al. Dynamic regulation of a ribosome rescue pathway in erythroid cells and platelets. Cell Rep. 2016;17(1):1–10.
[21] Fletcher SJ, Pisareva VP, Khan AO, et al. Role of the novel endoribonuclease SLFN14 and its disease-causing mutations in ribosomal degradation. RNA. 2018;24(7):939–949.
[22] Gao W, Wang K, Zhang L, et al. Pharmacological inhibition of S6K1 facilitates platelet activation by enhancing Akt phosphorylation. Platelets. 2019;30(2):241–250.
[23] Sundquist K, Ahmad A, Svensson PJ, et al. Polymorphisms in PARK2 and MRPL37 are associated with higher risk of recurrent venous thromboembolism in a sex-specific manner. J Thromb Thrombolysis. 2018;46(2):154–165.
[24] Deng HT, Liu HL, Zhai BB, et al. Vascular endothelial growth factor suppresses TNFSF15 production in endothelial cells by stimulating miR-31 and miR-20a expression via activation of Akt and Erk signals. FEBS Open Bio. 2016;7(1):108–117.
[25] Zhang K, Cai HX, Gao S, et al. TNFSF15 suppresses VEGF production in endothelial cells by stimulating miR-29b expression via activation of JNK-GATA3 signals. Oncotarget. 2016;7(43):69436–69449.
[26] Ergun S, Oztuzcu S. Sequence-based analysis of 5 UTR and coding regions of CASP3 in terms of miRSNPs and SNPs in targeting miRNAs. Comput Biol Chem. 2016;62:70–74.
[27] Della Bella S, Calcaterra F, Bacci M, et al. Pathologic up-regulation of TNFSF15-TNFRSF25 axis sustains endothelial dysfunction in unprovoked venous thromboembolism. Cardiovasc Res. 2020;116(3):698–707.
[28] Wang HW, Su SH, Wang YL, et al. MicroRNA-134 contributes to glucose-induced endothelial cell dysfunction and this effect can be reversed by far-infrared irradiation. PLoS One. 2016;11(1):e0147067.
[29] Lo WY, Peng CT, Wang HJ. MicroRNA-146a-5p mediates high glucose-induced endothelial inflammation via targeting interleukin-1 receptor-associated Kinase 1 expression. Front Physiol. 2017;8:551.
[30] Villasante A, Marturano-Kruik A, Ambati SR, et al. Recapitulating the size and cargo of tumor exosomes in a tissue-engineered model. Theranostics. 2016;6(8):1119–1130.
[31] Dieudé M, Bell C, Turgeon J, et al. The 20S proteasome core, active within apoptotic exosome-like vesicles, induces autoantibody production and accelerates rejection. Sci Transl Med. 2015;7(318):318ra200.
[32] Chyrchel B, Totoń-Żurańska J, Kruszelnicka O, et al. Association of plasma miR-223 and platelet reactivity

in patients with coronary artery disease on dual anti-platelet therapy: a preliminary report. Platelets. 2015;26 (6):593–597.

[33] Tan M, Yan HB, Li JN, et al. Thrombin stimulated platelet-derived exosomes inhibit platelet-derived growth factor receptor-beta expression in vascular smooth muscle cells. Cell Physiol Biochem. 2016;38 (6):2348–2365.